Elastic neutron scattering study of water dynamics in ion-exchanged type-*A* zeolites

C. Corsaro, V. Crupi, F. Longo, D. Majolino,* V. Venuti, and U. Wanderlingh
Physics Department, Messina University, c.da Papardo, S.ta Sperone 31, P.O. Box 55, 98166 S. Agata, Messina, Italy
(Received 28 July 2005; revised manuscript received 10 October 2005; published 20 December 2005)

With the aim to investigate, by means of elastic neutron scattering, the effects produced by the cation substitution on the dynamics of water in zeolites, we measured, using a neutron backscattering spectrometer, the temperature dependence of mean-square atomic displacements $\langle u^2 \rangle$ derived from window integrated quasielastic spectra of fully and partially hydrated Na-*A* and Mg50-*A* zeolites. The results, collected in the 20–273 K temperature range, reveal that, at low temperature, the $\langle u^2 \rangle$ shows a harmonic trend independent of hydration and cation substitution, and, at higher temperatures, the onset of a non-Gaussian dynamics of the elastic intensity. This latter takes place at $T \sim 200$ K and ~ 150 K for fully and partially hydrated samples, respectively. This behavior has been interpreted in terms of reorientational jumps of H atoms described by two-site processes within an asymmetric double-minimum potential. In spite of its simplicity, the model seems to reproduce the rearrangement of the hydrogen bond network of zeolitic water. The fit results indicate a reduced proton mobility by diminishing the water content and by the induced $Na^+ \rightarrow Mg^{2+}$ ion exchange, in agreement with previous incoherent quasielastic neutron scattering results at higher temperatures.

DOI: 10.1103/PhysRevE.72.061504 PACS number(s): 61.12.Ex, 61.43.Gt, 68.08.−p

I. INTRODUCTION

Nanoscopic confinement strongly alters, with respect to the bulk phase, the structure and dynamics of water, depending, among others, on the specific nature (hydrophobic or hydrophilic) of the substrate, the topology of the cavities, the hydration level and the temperature [1].

Nanoconfined water is found throughout in nature, from water in rocks and in biological cells to water entrapped in proteins and in membranes. Water in restricted geometry plays an important role in numerous chemical, geophysical, mineralogical, and biological processes [2,3]. As a result, an interest in the behavior of confined water has grown rapidly over the last decade, and widely demonstrated by the conspicuous literature existing in this field. The development of well characterized nanoporous, microporous, and mesoporous solids with a defined porous structure allowed a detailed description of the modified properties of the confined phase, by a systematic variation of the characteristic parameters of the substrate.

In view of the well-defined geometry, with a network of cylindrical pores, and the knowledge of surface details, Vycor and various types of silica glasses, with average pore diameters ranging from 15 to 100 Å, have been widely used as excellent prototypes of solid substrates in experiments performed with different techniques and also modeled by molecular dynamics (MD) simulation [4–11].

For these systems, experimental techniques and theoretical approaches evidenced an interfacial layer characterized by a hindered, slowed-down translational and rotational diffusion, together with a strong reduction of the hydrogen bond tetrahedral network. Another different layer, in the inner volume of the pore, is constituted by water molecules having structural and dynamical properties similar to the bulk phase. In this frame, previous light [12] and neutron [8] scattering studies allowed us to put into evidence the destructuring effects induced on interfacial water by confinement in 26 Å diameter pore of a sol-gel (GelSil) glass.

Thanks to their very strict distribution of pore dimensions and the high regularity of the crystalline structure, zeolites can be considered as ideal matrices for high selective, geometrically well-defined confinements in very narrow sizes, typically of the order of ~ 10 Å [13,14]. When the guest molecules, as in the present study, are water molecules, the subject may become particularly relevant. We expect, in fact, that, because of the severe confinement imposed by these materials, the physical properties of adsorbed water will be more affected with respect to, for example, Vycor or silica glasses. These studies will have, then, interesting fallout in the above mentioned biological fields. Moreover, they can be helpful in understanding the phase diagram of water, since the supercooled behavior, already found for water trapped in amorphous porous materials and phyllosilicates [15], can be maintained in a temperature range between 150 and 235 K.

A complete picture of structure and mobility of water molecules and zeolites framework and exchangeable cations, and the interaction between them, is still missing, even if it would be of paramount interest for synthesis and material science research, and it would require the use of sophisticated computer simulations combined with spectroscopic techniques.

Few experimental techniques are able to characterize local molecular motions within the channel or cavities of the zeolitic framework. Among them, NMR [16], Fourier transform IR (FT-IR) spectroscopy [17–19], and neutron scattering [20,21] have been proved to be powerful methods to obtain information on dynamical and geometrical aspects in molecular mobility.

In this paper, we present window integrated quasielastic spectra, obtained by an elastic neutron scattering (ENS) investigation, on fully and partially hydrated Na-*A*-type and Mg50-*A*-type zeolites. The results showed a departure from

*Corresponding author. Electronic address: majolino@unime.it

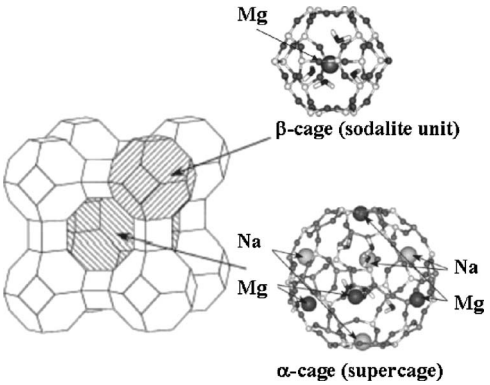

FIG. 1. Schematic representation of zeolite A framework, showing the α and β cages.

the Gaussian behavior of the elastic intensity, studied, as a function of temperature, in a wide experimental momentum transfer range.

The description of the observed dynamics is accounted by reorientational jumps of water molecules, reminiscing the rotational diffusion in the bulk phase. Information concerning the geometry and activation energies for the motion of protons are obtained by a simple model that treats the proton displacement in terms of jumps in a two minima potential profile with an energy difference of ΔE_a and separated by a distance d.

II. EXPERIMENT

Elastic neutron spectroscopy (ENS) measurements have been performed on syntethic zeolites *A* [or the sodium form of the Lynde type-*A* (Na-LTA) zeolite], as a function of temperature and hydration level.

In particular, hydrated powders of $Na_{12}[Al_{12}Si_{12}O_{48}]\cdot 27H_2O$ (Na-*A* zeolite) and $Mg_3Na_6[Al_{12}Si_{12}O_{48}]\cdot 33H_2O$ (Mg50-*A* zeolite, the expression of which indicates that the amount of Na^+ in the as synthesized Na-*A* zeolite is exchanged with the corresponding amount of Mg^{2+} by 50%) were used, without further purification, as purchased from Nippon Chemical Industrial Co., Ltd. These formulas are given for unit cells of fully hydrated materials, whose main properties can be found on the International Zeolite Association (IZA-SC) web site [22].

The well-recognized cage-type framework of zeolite *A* is reported in Fig. 1 [23]. The crystallographic structure is based on sodalitic units, cubo-octahedral in shape, of 24 SiO_4/AlO_4 tetrahedra linked together, called β cages. In it, six- and four-membered rings can be recognized. The interconnection, by oxygen bridges, at the double four-membered rings originates a new framework of bigger cavities connected together, the α cages, also called the supercage of zeolites *A*. Briefly, we can say that the *A* framework is constructed of α cages, arrayed in a simple cubic structure, by the sharing of the eight-membered rings. The eight-membered ring is called the window of the α cage, with an effective size of $\sim$4 Å. The effective inner size of the cage depends on the size of the cation, but nominally it is indicated roughly as 11 Å for the α cages and 7 Å for the β cages.

The channels and interconnected voids of the framework are occupied by the cation and water molecules. The cations are small enough to move through the pore system of the zeolite, and for this reason they may usually be exchanged by other cations. The water molecules in the zeolite channels are bonded by the forces of dipole interactions to the cations, forming their close surrounding. They also minimize the electrostatic repulsion between framework oxygens. Water molecules will also interact both with their water neighbors and with the zeolitic framework, always by H bond of comparable energy.

Furthermore, most of these water molecules can be removed reversibly on heating under vacuum the zeolite framework, leaving intact the crystalline host structure permeated by micropores and voids which may amount to as much as 50 vol % of the dehydrated crystals.

The pseudosymmetric structure of hydrated synthetic zeolite Na-*A* has been extensively refined, using single-crystal data, by Gramlich and Meier in 1971 [24]. Sodium and water position have been located.

The only cation site they identified with certainty is the position of Na(1) on the threefold axis near the center of the six-membered ring, tetrahedrally coordinated by four nearest neighbors, three framework oxygen atoms, and one H_2O molecule. The water molecules and the remaining sodium ions are distributed in five sites inside the zeolitic cavities. Up to five water molecules are located in site I inside the sodalitic units, generating a distorted tetrahedron. The α cages, where sites II and III are located, appears to be occupied by 20–22 H_2O molecules. The contents of site IV within the eight-membered ring windows provides the linkage between the water polyhedra. Finally, site V is revealed as a fairly broad peak at the center of the dodecahedral cluster, probably due to less symmetrical arrangements involving, possibly, one H_2O molecule and one Na^+ ion.

More recently, classical energy minimization techniques have been employed by Higgins *et al.* [25] to model the effects of hydration on the structures and on the adsorption behavior of extra-framework sodium and bivalent cations in zeolites *A*. The calculated structural parameters of a partially hydrated zeolite NaCa-*A*, a system perfectly analogous to our Mg50-*A* zeolite, appeared in full agreement with the experiments. Their calculations identified the β cage as the energetically preferred adsorption site for water molecules. These molecules are the most strongly adsorbed and, hence, will be retained within the zeolitic lattice even upon dehydration. The presence of water molecules is shown to strongly influence the most favorable positions of extra-framework cations that are calculated, for the siliceous structure, to be the α cage (in a six-ring window) for sodium ions, and the β cage (in a six-membered ring) for the bivalent ones, in agreement with experimental findings. In their preferred sites, sodium ions do retain up to five water molecules in their cluster, whereas bivalent cations are stabilized by four water molecules, arranged in tetrahedral coordination.

In the case of Na-*A* zeolites, then, the occupancy of sites of Na^+ cations inside the α cage will partially "reduce" the pore dimension. The Na^+ with Mg^{2+} ion exchange, on one

side, makes the number of ions in the zeolite diminish and, on the other side, "widens" the effective pore opening from ~4 to ~5 Å. In fact, bivalent ions prefer to locate inside the six-membered rings of the β cage, so leaving the entrance channels to zeolitic cavities free.

Partially hydrated samples were obtained from the fully hydrated ones by pumping at $T=200$ °C for two days. By the differences in weight, we evaluated the number of left water molecules. They turned out to be 18 for Na-*A* zeolite and 24 for Mg50-*A*.

For these measurements the backscattering spectrometer IN13 at the ILL facility was used to perform incoherent elastic neutron scattering scans, with a transferred momentum ranging from $Q=0.2$ to $Q=4.7$ Å^{-1}. The instrument was improved at low Q by a new set of circular array detectors. The instrumental resolution of $\Delta E=4$ μeV [half width at half maximum (HWHM)] was determined by calibrating the instrument with vanadium. The corresponding neutron wavelength was $\lambda=2.23$ Å. The energy resolution and exchanged momentum range will correspond to time and space windows determined, respectively, by $1/\Delta E$ and $2\pi/Q$. In our case, the instrumental resolution corresponds to a time window for accessible motion of $\leqslant$150 ps, in a spatial region with dimensions from ~30 to ~2 Å. In order to prevent the evaporation of water content, the powders were mounted in a thin-walled aluminum sachet which was contained in an indium sealed aluminum cell with internal spacing, in the case of fully hydrated zeolites, of 0.5 mm, placed at an angle of 135° to the incident beam. For both Na-*A* and Mg50-*A* zeolites in full hydration conditions, we used ~1.1 g of sample, in order to have a transmission of about 90%, so avoiding multiple scattering or multiphonon corrections. For partially hydrated samples, the thickness was properly increased in order to maintain a transmission of ~90%.

The temperatures explored ranged from 20 to 273 K. The check for the sample integrity was made by several scans up and down in temperature.

By using the software package ELASCAN available at ILL, the data were corrected to take into account for incident flux, cell scattering, self-shielding and detector response, and normalized to the sample at the lowest temperature ($T=20$ K). In this way, the coherent contribution arising from zeolite and water structure was removed.

III. RESULTS AND DISCUSSION

The aim of a neutron scattering experiment is to probe the functional dependence, on ω and Q, of the measured dynamical structure factor $S(Q,\omega)$, therefore providing information on the characteristic times and geometry of the molecular motions [26]. Moreover, as it is well known, with neutron scattering, it is possible to study both interparticle and self-particle correlations of collective or individual atomic motions. They are responsible, respectively, of the coherent and incoherent contributions to the scattering. Because of their large incoherent scattering cross section, the motions of hydrogen atoms dominate the observations. Moreover, in strong confinement, as in our case, the collective dynamics is expected to be damped. Thus, one is measuring the incoherent structure factor $S_{\mathrm{inc}}(Q,\omega)$, proportional to the cross-section in the Born approximation for N identical nuclei (H in our case) [27]. $S_{\mathrm{inc}}(Q,\omega)$ turns out to be the Fourier transform of the Van Hove self-correlation function $G_s(r,t)$, which in the case of translationally invariant systems is a function of the scalar distance r and time t.

According to literature [28–32], the low energy dynamical structure factor for Na-*A* and Mg50-*A* zeolites, in the incoherent approximation, can be written as

$$S_{inc}(Q,\omega) \propto e^{-Q^2\langle u^2\rangle}\{[A_t(Q)\,\delta(\omega)+(1-A_t(Q))L_t(\omega,\Gamma_t)] \otimes [A_r(Q)\,\delta(\omega)+(1-A_r(Q))L_r(\omega,\Gamma_r)]\} \quad (1)$$

as far as zeolitic water is concerned, plus another narrow δ line (that we did not report for simplicity) taking into account the zeolitic framework (6% of the total cross-section, as previously calculated [21]).

In the second term of the above-mentioned expression, $e^{-Q^2\langle u^2\rangle}$ is the so-called Debye Waller factor (DWF), which accounts for the decrease of the quasielastic intensity due to the vibrational atomic mean-square displacement $\langle u^2\rangle$. The first factor of the product is the translational component of water molecules. It consists of an elastic contribution (a δ line) typical of confinement, with a fractional area given by the elastic incoherent structure factor $A_t(Q)$, and a quasielastic line, Lorentzian in character, with a linewidth Γ_t and a fractional area 1-$A_t(Q)$. $A_t(Q)$ represents the Fourier transform of the spatial region where the dynamics is confined, so giving information on the spatial extent of confinement. Considering the topology of the zeolitic framework, we can assume a confined dynamics into a sphere of radius a, with an $A_t(Q)$ given by

$$A_t(Q)=\left[\frac{3j_1(Qa)}{Qa}\right]^2 \quad (2)$$

with j_1 spherical Bessel function of the first kind of order 1. In principle, the dimension of confinement a can be equal to the typical cavity size, even if many experimental results [4,8] indicated smaller values of the radius of the confining region. Actually, the confinement $L(\omega,\Gamma_t)$, describes, by the evolution of Γ_t as a function of Q, the dynamics that takes place inside the confinement region. In the same way, the second factor of Eq. (1) represents the rotational component of water molecules, also described by the weighted superposition of an elastic peak, a δ line with a fractional area $A_r(Q)$, and a quasielastic Lorentzian contribution, with a linewidth Γ_r and a fractional area $1-A_r(Q)$. In fact, the rotational motions of the protons relative to the center of mass also represent a kind of confined dynamics [28]: in particular, in the case of water, the rotation is due to the hydrogen atoms around the oxygens, and the confining region is a spherical shell of radius $b\sim0.9$ Å (the O-H bond length). In this case,

$$A_r(Q)=j_0(Qb)^2, \quad (3)$$

where j_0 is the spherical Bessel function of the first kind of order zero.

Theoretically, in our operative conditions, we single out the elastically scattered intensity $S(Q,\omega=0)$ as a function of

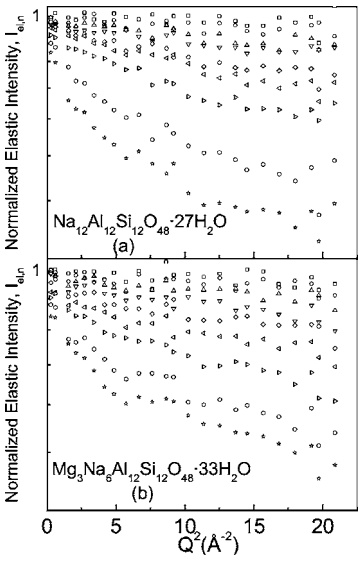

FIG. 2. Lin-log$_{10}$ plot of the normalized elastic intensity $I_{n\text{-}el}(Q)$ vs Q^2 for $Na_{12}Al_{12}Si_{12}O_{48}\cdot 27H_2O$ (a) and $Mg_3Na_6Al_{12}Si_{12}O_{48}\cdot 33H_2O$ (b) zeolites at $T=50$ K (squares), 80 K (circles), 110 K (up triangles), 140 K (down triangles), 170 K (rhombi), 200 K (left triangles), 230 K (right triangles), 260 K (diamonds), 273 K (stars).

both Q and T. Thus, in Eq. (1), only the convolution of the δ lines, weighted by their corresponding elastic incoherent structure factor, will survive.

On the other hand, the elastic intensity is related to the spatial Fourier transform of the limiting value of the $G(r,t)$ at $t\rightarrow\infty$. This will account for all the localized dynamics, like the Debye Waller factor, rotational motions, and confined diffusion, affecting both the coherent and incoherent scattering.

Actually, in the real experiment, the energy window has a finite width of ± 4 μeV, and this implies that slow dynamics ($t\sim 1/Q^2D>150$ ps) will be also measured as elastic intensity. This is the case for the translational contribution $L_t(\omega,\Gamma_t)$, since the typical diffusion coefficient is found to be of the order of $\sim 10^{-11}$ m^2/sec. As a consequence, the translational part in Eq. (1) becomes equal to unity.

Then, we'll be only concerned with vibrational and rotational contributions. We expect that at very low T, vibrational modes, expressed by the DWF, will play the main role.

In fact, a linear dependence is revealed in the lin-log$_{10}$ plot of the normalized elastic intensity $I_{\mathrm{el},n}$ vs Q^2, at $T<200$ K. It can be immediately observed, from an inspection of Fig. 2, in the case of fully hydrated samples, as an example. This indicates that, below this critical temperature, the dynamics of water molecules in zeolites is observed as purely vibrational, like a harmonic solid. This, of course, does not exclude the possibility of anharmonic motions at $T<200$ K, but such motions become slower than the experimental time scale. By increasing temperature, we observe a further decreasing of elastic intensity with a departure from the Gaussian trend, which has to be assigned to the activation of some kind of dynamics that should reflect the rotational term in Eq. (1).

On the other side, at low temperatures, the isotropic erratic rotation found in bulk water becomes more localized and it should be better accounted by some kind of reorientational jumps.

In this case, a reasonable model to describe the observed dynamics is the so-called double-well jump model. It was introduced some years ago by Stoeckly *et al.* [33], studying the H-bond dynamics of carboxylic acids and it is extensively applied to proton dynamics in several kinds of biomaterials [34,35].

An application of this model to our case can be attempted considering that, on one side, our spectra show a T dependence of the elastic intensity that closely recalls the above specified case. Moreover, the rotational form factor for water expressed by Eq. (3) is very close to 0 at $Q\sim 1$ Å^{-1}, while our experimental data clearly drop to 0 for much higher Q values (see Fig. 2). This occurrence also supports the existence of localized motions.

According to this model, the normalized elastic intensity $I_{\mathrm{el},n}(Q,T)$ is given by

$$I_n(Q,T)=F(T)\exp(-Q^2\langle u^2\rangle_G)\left\{1-2p_1p_2\left[1-\frac{\sin(Qd)}{Qd}\right]\right\} \tag{4}$$

in which $\langle u^2\rangle_G$ is the harmonic (Gaussian) contribution to the mean-square displacement, p_1 and $p_2=(1-p_1)$ are the occupation probabilities for two minima separated by a distance d. In the Q range, where $(Qd)^2$ is small compared to 1, the total mean-square displacement derived from Eq. (4) can be written as

$$\langle u^2\rangle_T=\langle u^2\rangle_G+\langle u^2\rangle_j=\langle u^2\rangle_G+\frac{p_1p_2d^2}{3}, \tag{5}$$

i.e., the sum of a harmonic ($\langle u^2\rangle_G$) and an anharmonic (jump, $\langle u^2\rangle_j$) contribution.

The T dependence of the harmonic mean-square displacement can be described by an Einstein model of independent oscillators [36]:

$$\langle u^2\rangle_G=\left(\frac{\hbar}{2M\omega_e}\right)\coth\left(\frac{\hbar\omega_e}{2k_BT}\right)-\langle u_0^2\rangle, \tag{6}$$

where M and ω_e are an effective mass and an average frequency of the set of oscillators, and $\langle u_0^2\rangle=\hbar/2M\omega_e$ is the mean-square displacement at $T=20$ K.

The spectra from the temperature scans have been so fitted all at once, using, as free parameters, $p_1(T)$ (having a different value for each temperature), M, ω_e, and d (having a common value for all temperatures). Moreover, a multiplicative T-dependent factor $F(T)$ was necessary, since the scattered intensity scales with T.

The least-mean-square fits are reported in Fig. 3 for full and partially hydrated samples at all the analyzed temperatures.

Concerning the harmonic contribution, the extracted values for the effective mass M, the average energy $\eta\omega_e$, and the atomic mean-square displacement $\langle u_0^2\rangle$ are reported in Table I. The behavior of the harmonic mean-square displacement $\langle u^2\rangle_G$ vs T is shown in Fig. 4 for all the analyzed samples. The obtained values of the effective mass M are

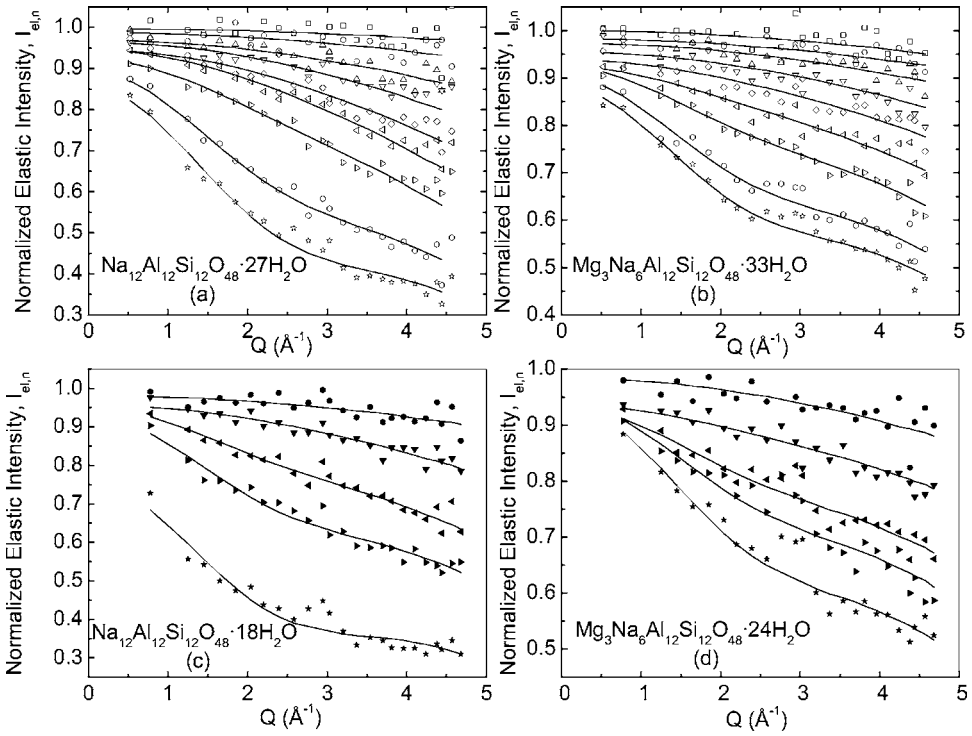

FIG. 3. Normalized elastic intensity $I_{n,el}(Q)$ vs Q for $Na_{12}Al_{12}Si_{12}O_{48}\cdot 27H_2O$ (a), $Mg_3Na_6Al_{12}Si_{12}O_{48}\cdot 33H_2O$ (b), $Na_{12}Al_{12}Si_{12}O_{48}\cdot 18H_2O$ (c), and $Mg_3Na_6Al_{12}Si_{12}O_{48}\cdot 24H_2O$ (d) at $T=50$ K (squares), 80 K (circles), 110 K (up triangles), 140 K (down triangles), 170 K (rhombi), 200 K (left triangles), 230 K (right triangles), 260 K (diamonds), 273 K (stars). Open symbols refer to fully hydrated samples, closed symbols refer to partially hydrated samples. Continuous lines are the least-mean-square fits performed by Eq. (4).

realistic and scale with the molar fraction of the solute ions.

For both full and partially hydrated samples, the found value of the average oscillators frequency ω_e indicates a stiffer H-bond network in the case of Mg50-*A* zeolite with respect to Na-*A* type. This occurrence is in agreement with a lower water mobility revealed by our recent incoherent quasielastic neutron scattering (IQENS) data [37]. These last results, in fact, gave evidence, as a consequence of the partial substitution, in Na-*A* zeolite, of monovalent Na^+ ions with Mg^{2+} bivalent ions, of a well-defined decrease of mobile water molecules, as revealed from the fraction f of immobile protons. In particular, we estimated, in the case of Na-*A* zeolite, 14 (at $T=293$ K) and 19 (at $T=333$ K) diffusing H_2O molecules, while, for Mg50-*A*, their number is decreased to 10 (at T=293 K) and 13 (at $T=333$ K). Such a behavior was explained in terms of a balance among the increased available volume for mobile H_2O molecules after the partial monovalent-bivalent cations substitution, considering the reduced number of extra-framework cations and the different positioning of bivalent Mg^{2+} ions reported in the Sec. II, and the higher electronegativity and smaller ionic radius of Mg^{2+} with respect to Na^+ ions.

TABLE I. Values for the effective mass M, the average energy $\hbar\omega_e$, and the atomic mean-square displacement $\langle u_0^2\rangle$ for all the analyzed samples.

Sample	M (amu)	$\hbar\omega_e$ (meV)	$\langle u_0^2\rangle$ Å^2
$Na_{12}Al_{12}Si_{12}O_{48}\cdot 27H_2O$	4.0±0.4	23±2	0.022±0.002
$Mg_3Na_6Al_{12}Si_{12}O_{48}\cdot 33H_2O$	2.3±0.2	33±3	0.025±0.002
$Na_{12}Al_{12}Si_{12}O_{48}\cdot 18H_2O$	3.4±0.3	26±2	0.021±0.002
$Mg_3Na_6Al_{12}Si_{12}O_{48}\cdot 24H_2O$	1.9±0.2	38±3	0.025±0.002

In addition, passing, for the same sample, from full to partial hydration, the oscillation energy slightly increases, while the effective mass tends to diminish. Even if the variations are not so relevant with respect to the experimental error, they can be justified thinking that water molecules removed by the dehydration process are the ones exhibiting the weakest bonds, and the remaining are expected to form a stiffer network with an increased average oscillation frequency but with an overall reduction of the effective mass.

As far as the anharmonic part is concerned, Fig. 4 also shows the behavior of the total mean-square displacements ($\langle u^2\rangle_T$) for both fully and partially hydrated Na-*A* and Mg50-*A* zeolites.

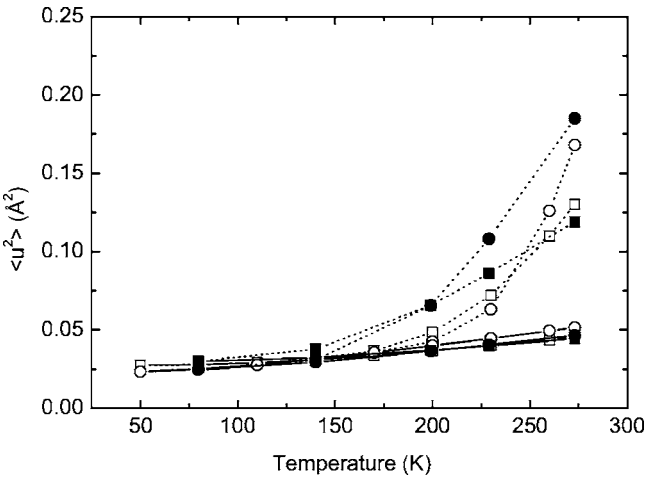

FIG. 4. Temperature dependence of $\langle u^2\rangle_T$ [dashed lines, fits by Eq. (5)] and $\langle u^2\rangle_G$ [continuous lines, fits by Eq. (6)] for $Na_{12}Al_{12}Si_{12}O_{48}\cdot 27H_2O$ (open circles), $Mg_3Na_6Al_{12}Si_{12}O_{48}\cdot 33H_2O$ (open squares), $Na_{12}Al_{12}Si_{12}O_{48}\cdot 18H_2O$ (closed circles), and $Mg_3Na_6Al_{12}Si_{12}O_{48}\cdot 24H_2O$ (closed squares).

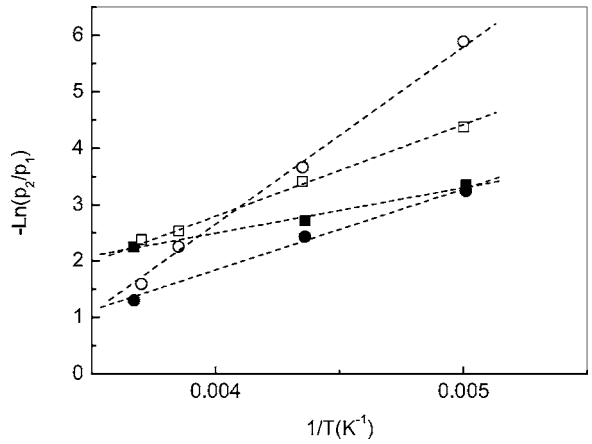

FIG. 5. Arrhenius plot of $-\ln(p_2/p_1)$ for $Na_{12}Al_{12}Si_{12}O_{48}\cdot 27H_2O$ (open circles), $Mg_3Na_6Al_{12}Si_{12}O_{48}\cdot 33H_2O$ (open squares), $Na_{12}Al_{12}Si_{12}O_{48}\cdot 18H_2O$ (closed circles), and $Mg_3Na_6Al_{12}Si_{12}O_{48}\cdot 24H_2O$ (closed squares).

In the case of fully hydrated samples, it is seen that the onset of the anharmonic diffusive dynamics occurs for both samples at a temperature of about 200 K. In addition, $\langle u^2\rangle_T$ for Na-*A* zeolite increases, with increasing T, more rapidly with respect to Mg50-*A* zeolite.

For partially hydrated samples, the observed anharmonic onset occurs at $T\cong 150$ K. Also in this case, $\langle u^2\rangle_T$ for Na-*A* zeolite grows with T more rapidly than in Mg50-*A* case, as in full hydrated samples. This occurrence confirms, in full agreement with our previous cited IQENS results on the same samples at full hydration and higher temperatures [37], a greater mobility for H_2O molecules in Na-*A* zeolites than Mg50-*A* type.

The observed lowering of the onset temperature, of about 50 K, suggests a smaller activation energy for partially hydrated samples.

Anyway, more detailed information on the activation energy can be obtained by studying the T dependence of the average occupation probabilities p_1 and p_2.

In our case p_1 and p_2 extracted from the fit turned out to follow an Arrhenius behavior (see Fig. 5),

$$\frac{p_2}{p_1} = \exp\left(\frac{-\Delta E_a}{RT}\right), \tag{7}$$

in which E_a represents the height of the energy barrier and R is the gas constant.

As it is well known, at constant temperature and pressure $\Delta E_a = \Delta H - T\Delta S$. So, ΔH and ΔS can be extracted, respectively, from the slope and the intercept of the linear variation of the curve $-\ln(p_2/p_1)$ vs $1/T$. The so-obtained values are reported in Table II.

For both fully and partially hydrated samples, the obtained ΔH contribution to the energy barrier is higher for Na-*A* zeolite. This may lead to a reduced mobility, but it widely compensated by the entropic term at high T.

Within the framework of the double-well model, the present findings suggest that reducing the water molecules in the same sample causes a lowering of the energy barrier for this reorientational transition. A qualitative explanation to this experimental evidence could be given taking into account that, as specified in the experimental section, dehydration causes, for both samples, a reduction of ~35% of the number of H_2O molecules in the α cage. As a consequence, the molecular rearrangement would involve a reduced number of H bonds to be broken, which will be reflected in a small activation energy. The increased available volume after dehydration may also justify the reduced entropic contribution values, since in this case, fully developed ordered structures are more likely to take place.

TABLE II. Values for the enthalpic (ΔH) and entropic ($\Delta S/R$) contribution to the energy barrier, and the jump length d for all the investigated samples.

Sample	ΔH (kJ/mol)	$\Delta S/R$	d (Å)
$Na_{12}Al_{12}Si_{12}O_{48}\cdot 27H_2O$	26±3	10±1	1.6±0.2
$Mg_3Na_6Al_{12}Si_{12}O_{48}\cdot 33H_2O$	13±1	3.7±0.4	1.7±0.2
$Na_{12}Al_{12}Si_{12}O_{48}\cdot 18H_2O$	12±1	3.9±0.4	1.6±0.2
$Mg_3Na_6Al_{12}Si_{12}O_{48}\cdot 24H_2O$	6.7±0.7	0.7±0.1	1.6±0.2

Finally, we remark that the obtained ΔE_a values turned out to be a few tens of kJ, i.e., the same order of magnitude of the H-bond average energy.

The obtained jump length d, turned out to be ~1.6 Å in all cases (see Table II). This value is exactly the H···H distance in water molecules, confirming once again the validity of the hypothesis of a localized reorientational jump.

IV. CONCLUSIONS

The water dynamics in ~10 Å voids of Na-*A* and Mg50-*A* zeolites has been investigated by elastic neutron spectroscopy, as a function of temperature, water content, and cation substitution.

The adsorbed water appears to behave, within the experimental time window ($\tau \leqslant 150$ ps), like a harmonic solid up to a given temperature T^* that is independent of the cation substitution, but depending on the hydration percentage. T^* turned out to be ~200 K and ~150 K for fully and partially hydrated samples, respectively.

Afterward, an anharmonic H-bond dynamics is smoothly activated by a process which can be described by a two-site jump model. Since the observed jump distance turned out to be for all sample equal to the H···H distance in water molecule, we interpret the observed dynamics as a reorientational motion of H_2O molecules in a rearranging H-bond network. The extracted activation energies for this dynamics are consistent with the breaking of few hydrogen bonds.

For both fully and partially hydrated samples, the partial exchange of Na^+ ions with Mg^{2+} is found to give rise to a reduced mobility of H_2O molecules.

ACKNOWLEDGMENT

The ILL Scientific Coordination Office (SCO) is acknowledged for the dedicated beam time.

[1] B. Webber and J. Dore, J. Phys.: Condens. Matter **16**, S5449 (2004).
[2] G. Sartor, A. Halbrucker, and E. Mayer, Biophys. J. **69**, 2679 (1995).
[3] J. A. Rupley and G. Careri, Adv. Protein Chem. **41**, 37 (1991).
[4] M. C. Bellissent-Funel, S. H. Chen, and J. M. Zanotti, Phys. Rev. E **51**, 4558 (1995).
[5] J. M. Zanotti, M. C. Bellissent-Funel, and S. H. Chen, Phys. Rev. E **59**, 3084 (1999).
[6] V. Crupi, D. Majolino, P. Migliardo, V. Venuti, and M. C. Bellissent-Funel, Mol. Phys. **101**, 3323 (2003).
[7] V. Crupi, A. J. Dianoux, D. Majolino, P. Migliardo, and V. Venuti, Phys. Chem. Chem. Phys. **4**, 2768 (2002).
[8] V. Crupi, D. Majolino, P. Migliardo, and V. Venuti, J. Phys. Chem. B **106**, 10884 (2002).
[9] F. Bruni, M. A. Ricci, and A. K. Soper, J. Chem. Phys. **109**, 1478 (1998).
[10] S. M. Alnaimi, J. Mitchell, J. H. Strange, and J. B. W. Webber, J. Chem. Phys. **120**, 2075 (2004).
[11] P. Gallo and M. Rovere, J. Phys.: Condens. Matter **15**, 7625 (2003).
[12] V. Crupi, S. Magazù, D. Majolino, G. Maisano, and P. Migliardo, J. Mol. Liq. **80**, 133 (1999).
[13] G. Gottardi and E. Galli, *Natural Zeolites* (Sprinter-Verlag, Berlin, 1985).
[14] R. M. Szostak, *Molecular Sieves* (Van Nostrand Reinhold, New York, 1989).
[15] J. Teixeira, J. M. Zanotti, M. C. Bellissent-Funel, and S. H. Chen, Physica B **370**, 234 (1997).
[16] I. A. Beta, B. Hunger, W. Böhlmann, and H. Jobic, Microporous Mesoporous Mater. **79**, 69 (2005).
[17] V. Crupi, D. Majolino, P. Migliardo, V. Venuti, and U. Wanderlingh, Eur. Phys. J. E **12**, S55 (2003).
[18] V. Crupi, D. Majolino, P. Migliardo, V. Venuti, and T. Mizota, Mol. Phys. **102**, 1943 (2004).
[19] V. Crupi, F. Longo, D. Majolino, and V. Venuti, J. Chem. Phys. **123**, 154072 (2005).
[20] R. Schenkel, A. Jentys, S. F. Parker, and J. A. Lercher, J. Phys. Chem. B **108**, 7902 (2004).
[21] V. Crupi, D. Majolino, P. Migliardo, V. Venuti, U. Wanderlingh, T. Mizota, and M. Telling, J. Phys. Chem. B **108**, 4314 (2004).
[22] Database of Zeolite Structure. http://www.iza-structure.org/databases/
[23] R. M. Barrer, *Zeolites and Clay Minerals as Sorbents and Molecular Sieves* (Academic Press, London, 1982).
[24] V. Gramlich and W. M. Meier, Z. Kristallogr. **133**, 134 (1971).
[25] F. M. Higgins, H. N. De Leeuw, and S. C. Parker, J. Mater. Chem. **12**, 124 (2002).
[26] M. Bèe, *Quasielastic Neutron Scattering* (Hilger, Bristol, 1988).
[27] W. Marshall and S. Lovesey, *Theory of Thermal Neutron Scattering* (Oxford University Press, London, 1971).
[28] S. H. Chen, in *Hydrogen-bonded Liquids*, edited by J. C. Dore and J. Teixeira (Kluwer Academic, Dordrecht, 1991).
[29] J. Teixeira, M. C. Bellissent-Funel, S. H. Chen, and A. J. Dianoux, Phys. Rev. A **31**, 1913 (1985).
[30] S. Yip, in *Spectroscopy in Biology and Chemistry, Neutron, X-ray, Laser*, edited by S. H. Chen and S. Yip (Academic, New York, 1974).
[31] A. Rahman and F. H. Stillinger, J. Chem. Phys. **55**, 3336 (1971).
[32] A. Rahman and F. H. Stillinger, J. Chem. Phys. **57**, 1281 (1972).
[33] A. Stoeckli, A. Furrer, C. Schoenenberger, B. H. Meier, R. R. Ernst, and I. Anderson, Physica B & C **136**, 161 (1986).
[34] U. N. Wanderlingh, C. Corsaro, R. L. Hayward, M. Bée, and H. D. Middendorf, Chem. Phys. **292**, 445 (2003).
[35] A. Paciaroni, S. Cinelli, and G. Onori, Biophys. J. **83**, 1157 (2002).
[36] J. C. Smith, Q. Rev. Biol. **24**, 1 (1991).
[37] C. Corsaro, V. Crupi, D. Majolino, P. Migliardo, V. Venuti, U. Wanderlingh, T. Mizota, and M. Telling Mol. Phys. (to be published).